Grating-coupled plasmonic sensor for sucrose sensing fabricated using optical fiber-based interference lithography (OFIL) system

Pae, Jian Yi; Sahoo, Pankaj Kumar; Murukeshan, Vadakke Matham

2019

Pae, J. Y., Sahoo, P. K., & Murukeshan, V. M. (2019). Grating-coupled plasmonic sensor for sucrose sensing fabricated using optical fiber-based interference lithography (OFIL) system. IEEE Sensors Journal, 19(22), 10477-10481. doi:10.1109/JSEN.2019.2933668

https://hdl.handle.net/10356/141000

https://doi.org/10.1109/JSEN.2019.2933668

Grating-coupled plasmonic sensor for sucrose sensing fabricated using optical fiber-based interference lithography (OFIL) system

Jian Yi Pae, Pankaj K. Sahoo, and Murukeshan Vadakke Matham

***Abstract*—A grating-coupled plasmonic sensor for sucrose sensing was fabricated and experimentally validated in the spectral interrogation mode. The grating structures were fabricated on a silicon wafer using an optical fiber-based interference lithography (OFIL) system. The system can be easily reconfigured to write 1D grating features with a periodicity ranging from 514 nm to 1,646 nm. The patterned area can also be controlled from 5 mm down to 0.6 mm for energy efficient, device scale fabrication. The results demonstrated the potential of using the OFIL system as a highly versatile and low-cost method to fabricate grating-coupled plasmonic sensors for healthcare applications.**

***Index Terms*—Biosensors, interferometric lithography, optical fibers, optical sensors, plasmons**

I. Introduction

Interference lithography (IL) techniques have long played an important role in the fabrication of nanoscale features with a wide variety of applications [1]–[4]. The major benefit of IL over other conventional nanofabrication techniques is the relative ease in generating large area 1D, 2D, or even 3D interference patterns [5]–[9] with relatively simple optical components. The interference patterns could then be recorded in a photoresist layer and transferred to other substrates or materials for a wide variety of applications such as photonic crystals, solar cells, high-density data storage devices and biosensors [10]–[13].

Various methods can be adapted to split a single coherent light beam into multiple sub-beams necessary for generating the desired interference pattern [14], [15]. Conventionally, beam splitting is achieved by using beam splitters or partially reflecting mirrors [16]. However, such systems, when set up in free-space, can be quite challenging to align due to the sheer number of optical components and optomechanical mounts [17]. This creates a major concern as the optical path difference between the sub-beams needs to maintain within the coherence length of the light source for interference to occur. This problem becomes more evident when forming interference patterns from multiple beams to fabricate highly complex structures [18].

Recently, single-input/multiple-output (SIMO) optical fibers have also been demonstrated as an alternative approach for IL [19]. The SIMO optical fiber would serve the purpose of a beam splitter as well as provide a flexible medium for beam delivery. The main benefit of this is that the end faces of the optical fiber can be repositioned easily for delivery of the sub-beams at a desired angle of incidence without the use of mirrors or reflectors. In addition, the polarization of each of the sub-beams can also be controlled independently to maximize the contrast of the pattern [20]. Hence, an optical fiber-based interference lithography (OFIL) system would greatly enhance the versatility of an IL system and greatly reduce its complexity.

In this paper, a 2-beam OFIL system is developed for fabricating the nanoscale 1D grating features for plasmonic-based sensing applications. The advantage of the developed OFIL system is that the 2 end faces of the optical fiber are mounted on rotation stages that are aligned on the same rotation axis, hence, the angle of incidence of the sub-beams can be varied easily with minimal realignment or adjustment for fabricating 1D grating features with different periodicities. In addition, the use of a fiber collimation package allows the laser spot diameter to be confined to only the targeted pattern area so as to maximize the laser energy efficiency in writing the interference pattern.

After the grating features are fabricated, it is then developed into a gold grating coupled plasmonic sensor and its potential as a biosensor for sucrose sensing was demonstrated. It is envisioned that the OFIL system could be easily integrated with other micro and nanoscale fabrication processes which would allow greater versatility and efficiency in the fabrication of micro–nanoscale features for the mass production of photonics devices, such as optical sensors and lab-on-a-chip devices for medical and healthcare applications.

Manuscript received May 30, 2019. This work was supported in part by MOE Tier 1 Grant RG192/17. MVM and PKS acknowledge the EDB-IPP, PFSAP-SC3DP project for the funding support. JYP acknowledge NTU for the Research Student Scholarship and SC3DP which is supported by the National Research Foundation, Prime Minister's Office, Singapore under its Medium-Sized Centre funding scheme. *(corresponding author: Murukeshan V. M.)*

J. Y. Pae and Murukeshan V. M. are with the Singapore Centre for 3D Printing (SC3DP) and Center for Optical and Laser Engineering (COLE), Nanyang Technological University (NTU), Singapore 639798 (e-mail: paej0001@e.ntu.edu.sg; mmurukeshan@ntu.edu.sg).

Pankaj K. S. was with NTU, Singapore and is currently with Center for Imaging Science, Rochester Institute of Technology (RIT), NY 14623, USA (e-mail: 8pankaj8@gmail.com).

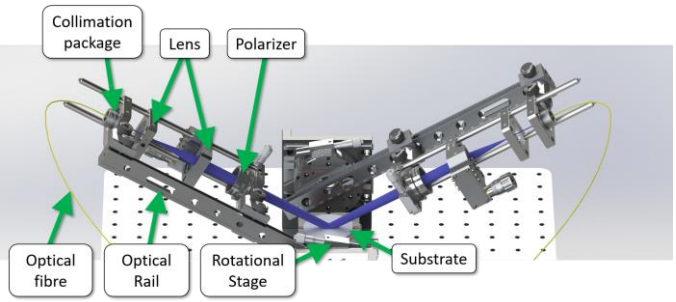

Fig. 1. Schematic model of the optical fiber interference lithography system (laser beam path is illustrated in blue).

II. OFIL System

The schematic model of the proposed OFIL system is shown in Fig. 1. A diode-pumped solid-state (DPSS) laser (CNI Co., Ltd.) with 405 nm emission wavelength is selected as the light source whose long coherence length (>1 m) is ideal for IL. The optical fiber is designed to be single-mode for 405 nm and the input end is split, using a custom-fabricated fused fiber splitter (FONT Co.), into two output ends with a 50:50 splitting ratio. The input end is first mounted on a fiber launch system with 3-axis adjustability to ensure maximum coupling of laser light into the optical fiber. A 0.10 NA 4X microscope objective (Olympus Corp.) is also used to tightly focus the laser light into the optical fiber. Each of the output ends is then mounted on separate optical rails which are attached to individual rotation stages that are aligned on the same rotation axis. Therefore, the interference plane would always be at the same distance from the fiber output end regardless of the rotation angle which reduces the need to realign the laser beam after each adjustment. A 3-axis sample holder is then added to position the substrate at the interference plane for recording the interference pattern.

TABLE I
Required angle of incidence for the targeted periodicity and the actual measured periodicity.

Targeted periodicity, Λ_t (nm)	Required angle of incidence, θ	Measured periodicity, Λ_m (nm)
500	23.89°	514
1000	11.68°	980
1600	7.27°	1646

The optical components are mounted on a cage system to simplify the aligning process. In addition, different optical components, such as polarizers and lens, can be easily added to the system in a controlled way to reshape the beams for achieving the desired contrast, type of interference pattern and pattern area. In the system, a fiber collimator is attached directly to the fiber end face to collimate the laser beam and a series of plano-convex lenses are then used to expand the diameter of the sub-beams to approximately 5 mm. A polarizer is also added to ensure the sub-beams are s-polarized for the best contrast in the interference pattern.

Before recording the interference pattern, the output power from each end of the optical fiber is first measured using a power meter (PMA100A from Thorlabs, Inc.). The power in both sub-beams is then tuned using a 3-axis fiber launch system (Thorlabs, Inc.) and made to be equal at approximately 0.6 ± 0.05 mW. Considering the spot size of the beams, the intensity of each beam is calculated to be approximately 3.06 mW/cm^2. Therefore, the required exposure time necessary for patterning can be derived from the exposure dosage of the photoresist. A mechanical shutter, with a temporal resolution of 10 ms, is used to control the exposure time.

Next, a silicon (Si) wafer is prepared by spin-coating a layer of negative-tone photoresist (NR7-500P from Futurrex, Inc.) at 4,000 rpm over the surface. The photoresist is then soft baked at 150 °C for 60 s and cooled to room temperature before it is

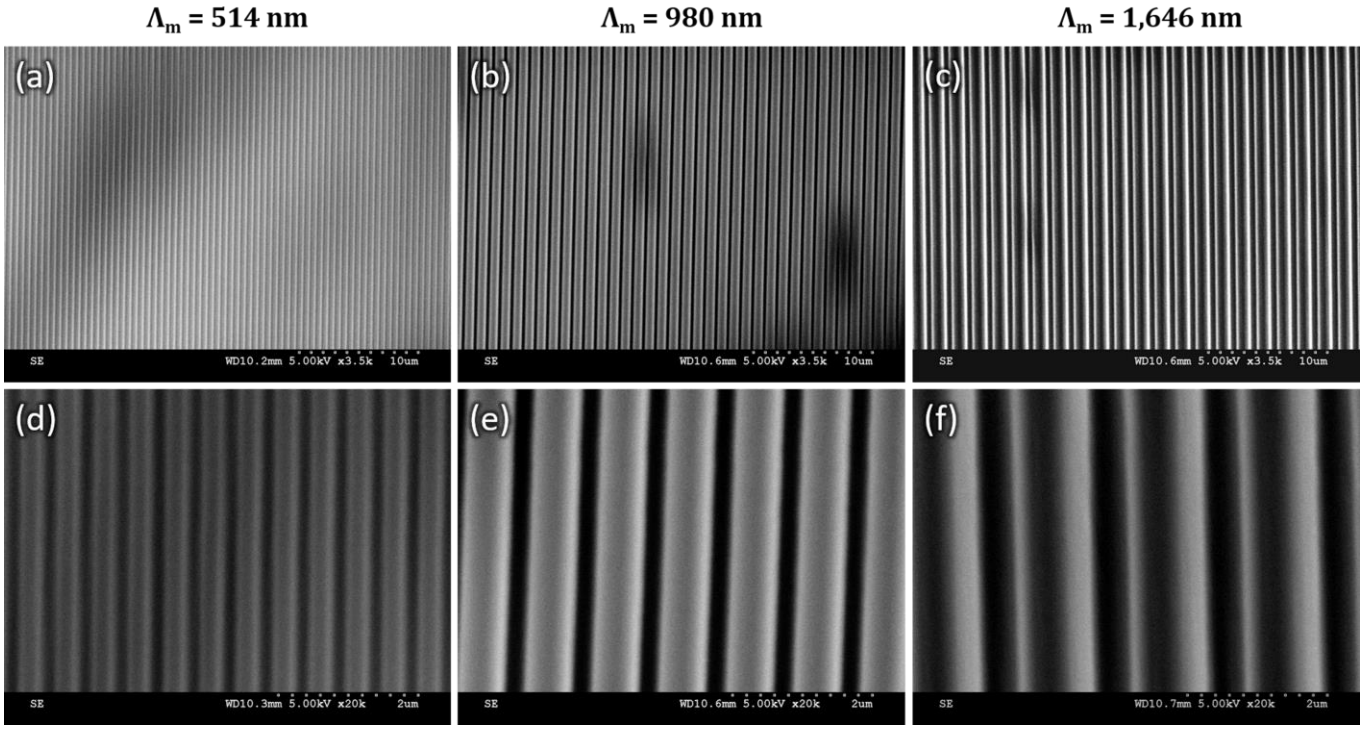

Fig. 2. SEM images of the respective grating features at (a)-(c) 3,500x and (d)-(f) 20,000x magnifications for the respective Λ_m.

mounted on the sample holder. After exposing the photoresist for 900 ms, the Si wafer is then baked at 100 °C for 60 s and developed in a diluted developer solution (RD6) for 1 min. The substrates are then inspected using scanning electron microscopy (SEM) to confirm its periodicity.

The versatility of this system is demonstrated by fabricating 1D grating features with different periodicities by rotating the optical rails to realize different angles of incidence. For a simple 2-beam IL system, the resulting periodicity of the interference pattern is described as $\Lambda_t = \lambda / 2 \sin\theta$ [21], where λ is the wavelength of the laser light and θ is the angle of incidence. Table 1 shows the targeted periodicity (Λ_t) in the interference pattern and the required angle of incidence. The measured periodicity (Λ_m) of the fabricated 1D grating features is also given in the last column for comparison purposes. These values are calculated by analyzing the line profile plot of the SEM images.

The SEM images of the different 1D grating features and their respective targeted periodicity are shown in Fig. 2. The top 3 images show the features at 3,500x magnification while the bottom 3 images are at 20,000x magnification. The grating features are observed throughout the entire patterned area and have good contrast. Therefore, this demonstrates the versatility of using the optical fiber IL system to fabricate a wide range of nanoscale and microscale grating features.

The Λ_m is calculated from the line profile plot measured from the SEM images using an image processing software (ImageJ). After image filtering, the individual peaks are identified based on the maximum relative grayscale intensity values and Λ_m can be calculated by taking the average of their respective peak-to-peak value. As shown in Fig. 3, the line profile plot of the sample with Λ_t of 500 nm, corresponding to Fig. 2 (a), is plotted in terms of its grayscale intensity. The measured periodicity of the 1D grating features agrees well with the values derived using the theoretical formula. The difference in the two values can be attributed to the zero error with respect to the interference plane and due to the accuracy of the rotation stage (1° resolution). This error can possibly be minimized by using a stepper motor for more precise control of the rotation stage. This demonstrates the potential of the optical fiber IL as a highly versatile method for the fabrication of grating features with different periodicities.

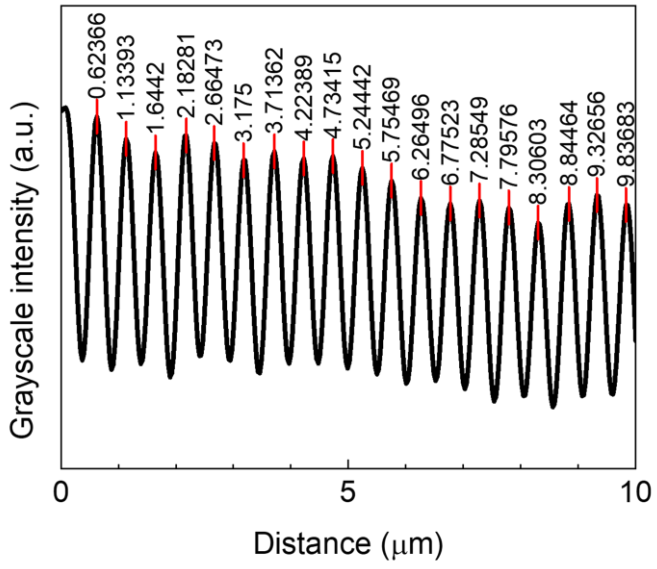

Fig. 3. Line profile plot of the sample with 500 nm targeted periodicity

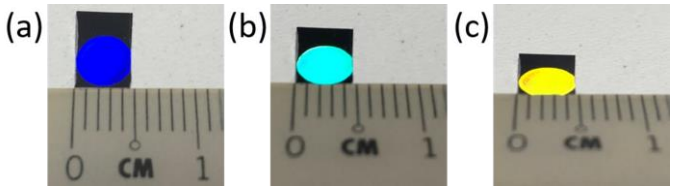

Fig. 4. Actual image of the samples showing different colors at a viewing angle of approximately (a) 10°, (b) 45° and, (c) 80°

Fig. 4 shows the actual images of the 500 nm periodicity grating sample when viewed from different angles. As can be seen from the images, the reflected light changes color from blue to yellow when the viewing angle is increased. This is due to the diffraction of white light when it is reflected off the grating features. This method allows us to quickly verify and confirm the successful patterning of the grating features without the need for any microscopy techniques.

III. Development of a Grating-Coupled Plasmonic Sensor

In order to demonstrate the potential of this system as a nanofabrication tool, 1D gold gratings with 500 nm periodicity are fabricated for the development of a grating-coupled plasmonic sensor. Surface plasmon (SP) is described as a collective oscillation of free electrons at a metal-dielectric interface [22], [23]. The SP propagates along the interface and can be excited with an external transverse-magnetic (TM) electromagnetic wave if they have the same propagation vector [24]. This can be achieved with a metallic diffraction grating when the following condition is satisfied [25].

$$k_0 n_d \sin(\theta) + m\frac{2\pi}{\Lambda} = \pm \mathrm{Re}(k_{SP}) \quad (1)$$

Here k_0 is the propagation constant in vacuum, n_d is the refractive index of the dielectric medium, θ is the angle of incidence of the light on the diffraction grating, m is the diffraction order, Λ is the periodicity of the grating and k_{SP} is the propagation vector of the SP wave. When the above condition is satisfied, there is a resonant coupling of energy transfer from the incident light to the SP which would result in a drop in the reflected energy [26]. Therefore, by observing the spectrum of the reflected light, we can identify the resonance wavelength as a sharp dip [27], [28]. Since k_{SP} is governed by the refractive index of the dielectric medium, therefore, by monitoring the shift in the resonance wavelength, a plasmonic sensor can effectively function as a refractive index sensor [29].

A two-step lift-off process was used to fabricate the gold metallic diffraction grating features. First, a layer of gold is sputtered over the Si wafer followed by coating a layer of photoresist for recording the 1D grating interference pattern. Next, a second layer of gold is deposited over the patterned photoresist which fills the gaps in between the grating features. Subsequently, the photoresist is lift-off in an acetone bath

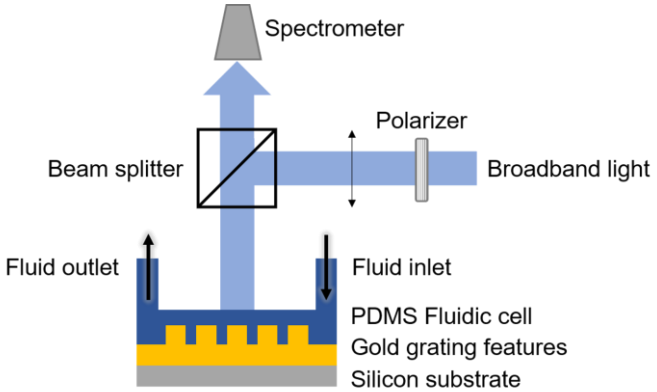

Fig. 5. Schematic illustration of the gold grating-coupled plasmonic biosensor configured for spectral interrogation mode.

leaving behind a gold grating pattern. The gold grating was then developed as a plasmonic sensor in the spectral interrogation mode as shown in Fig. 5. A broadband halogen light source is first collimated and directed through a polarizer and a beam splitter to incident TM polarized light normally to the surface of the gold grating. The reflected light from the gold grating is then collected by a collector lens which is coupled to a spectrometer (USB4000, Ocean Optics, Inc.). The fluidic cell is formed using polydimethylsiloxane (PDMS) which covers the surface of the gold grating [30]. The sample dielectric fluid is then injected into the fluidic chamber through the inlet and outlet of the fluidic cell and the reflection spectrum of the sample is analyzed using the spectrometer.

Fluids with different concentrations of sucrose were then introduced into the fluidic cell which covers the surface of the grating and the measured reflection spectra are shown in Fig. 6a. From the figure, a sharp dip in the reflection spectra is clearly observed, at the resonance wavelength for all the sample fluids and there is a red shift with increasing sucrose concentration. This confirms that the sucrose concentration has a direct effect on the refractive index of the sample fluid which would affect the resonance condition at the metallic-dielectric interface formed by the gold and sucrose fluid. The respective sucrose concentration values were then converted into molar concentration (M) and then plotted with the observed resonance wavelength as shown in Fig. 6b to establish the relationship between the two values. From this, the sensitivity of the plasmonic sensor can be estimated from the linear fit to be 13.1 ± 0.5 nm/M and the detection limit of the system is calculated to be 16.61 mM.

In order to confirm that the reflectance is indeed due to the plasmonic effect, a controlled experiment was also performed by recording the reflection spectrum with s-polarized light. There is no distinctive drop in the reflectance which suggests that there is no resonant coupling of light to the excite the surface plasmons. This is because the polarization direction is orthogonal to the grating direction and therefore, the incident light could not be coupled to the interface for excitation of the SP.

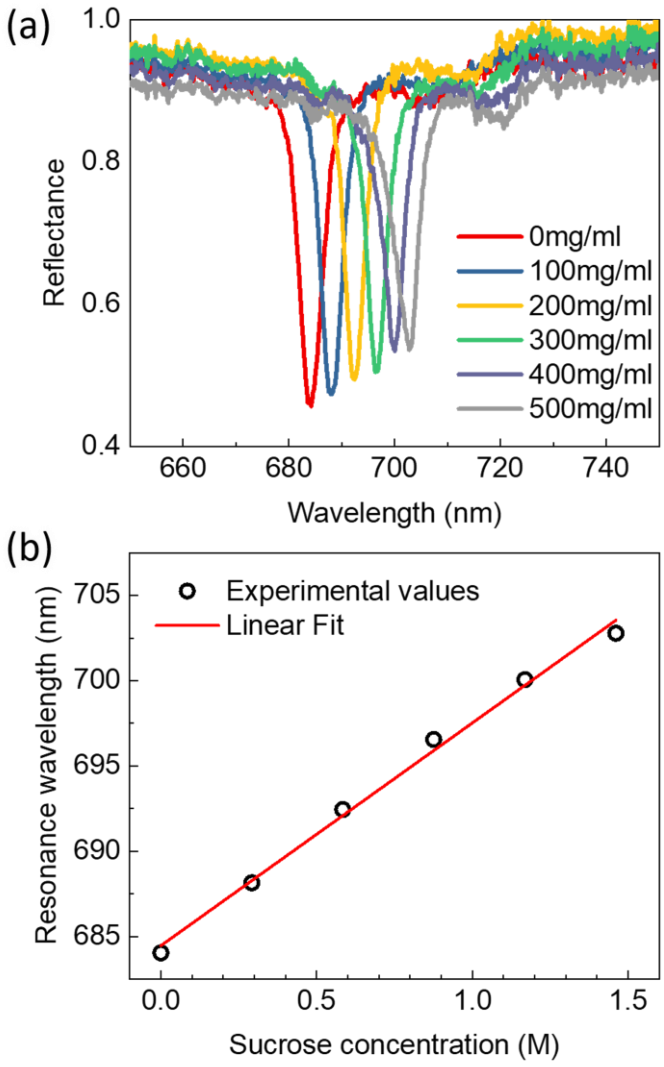

Fig. 6. (a) Spectrum of the reflected light collected by the spectrometer for each sucrose concentration, (b) plot of the observed resonance wavelength against the respective refractive index of the sucrose solutions

IV. Conclusion

An optical fiber-based IL system offers the benefits of flexibility and reduced complexity as compared to conventional IL systems. In this paper, we demonstrated the versatility and robustness of the configured OFIL system to fabricate interference patterns of approximately 5 mm diameter with multiple periodicities ranging from 514 nm to 1,646 nm. The patterned area could also be easily varied by adjusting the distance between the lens or using a lens with different focal length without affecting the alignment of the laser beams. As a result, the time needed to readjust and realign the optics for realizing different interference pattern or a specific design is significantly reduced. Additionally, a more energy efficient fabrication process is realized as the laser beam is expanded only to the desired pattern area with minimal losses as the unnecessary regions are not patterned. Therefore, it is envisioned that the OFIL system allows for a more efficient approach to realize a multitude of micro-nanoscale periodic features with optimized designs and geometries for specific

device scale fabrication such as the demonstrated plasmonic sensor.

REFERENCES

[1] Y. Yang, Q. Li, and G. P. Wang, "Design and fabrication of diverse metamaterial structures by holographic lithography," *Opt. Express*, vol. 16, no. 15, pp. 11275–11280, 2008.

[2] J. K. Chua and V. M. Murukeshan, "Patterning of two-dimensional nanoscale features using grating-based multiple beams interference lithography," *Phys. Scr.*, vol. 80, no. 1, p. 015401, 2009.

[3] J. Choi *et al.*, "Investigation on Fabrication of Nanoscale Patterns Using Laser Interference Lithography," *J. Nanosci. Nanotechnol.*, vol. 11, no. 1, pp. 778–781, 2011.

[4] D. G. Kim *et al.*, "SPR properties of 2D ZnO nano-holes fabricated by laser interference lithography," *Electron. Lett.*, vol. 49, no. 8, pp. 551–552, Apr. 2013.

[5] S. Benoit and S. R. J. Brueck, "Design of Chirped Gratings Using Interferometric Lithography," *IEEE Photonics J.*, vol. 10, no. 2, pp. 1–13, Apr. 2018.

[6] K. . V. Sreekanth and V. M. Murukeshan, "Large-area maskless surface plasmon interference for one- and two-dimensional periodic nanoscale feature patterning," *J. Opt. Soc. Am. A*, vol. 27, no. 1, p. 95, 2010.

[7] D. S. Isakov, N. D. Kundikova, and Y. V. Miklyaev, "Interference lithography for the synthesis of three-dimensional lattices in SU-8: Interrelation between porosity, an exposure dose and a grating period," *Opt. Mater. (Amst).*, vol. 47, pp. 473–477, 2015.

[8] J.-H. Jang *et al.*, "3D Micro- and Nanostructures via Interference Lithography," *Adv. Funct. Mater.*, vol. 17, no. 16, pp. 3027–3041, Nov. 2007.

[9] J. W. Menezes, L. A. M. Barea, E. F. Chillcce, N. Frateschi, and L. Cescato, "Comparison of Plasmonic Arrays of Holes Recorded by Interference Lithography and Focused Ion Beam," *IEEE Photonics J.*, vol. 4, no. 2, pp. 544–551, Apr. 2012.

[10] R. Sidharthan, M. Kumar, J. Joseph, and V. M. Murukeshan, "Realization of body centered tetragonal, β-tin and diamond type structures using five beam interference," *Opt. Commun.*, vol. 322, pp. 160–163, 2014.

[11] A. P. Amalathas and M. M. Alkaisi, "Fabrication and Replication of Periodic Nanopyramid Structures by Laser Interference Lithography and UV Nanoimprint Lithography for Solar Cells Applications," in *Micro/Nanolithography - A Heuristic Aspect on the Enduring Technology*, M. M. A. E.-J. Thirumalai, Ed. Rijeka: IntechOpen, 2018, p. Ch. 2.

[12] Q. Xie, M. H. Hong, H. L. Tan, G. X. Chen, L. P. Shi, and T. C. Chong, "Fabrication of nanostructures with laser interference lithography," *J. Alloys Compd.*, vol. 449, no. 1, pp. 261–264, 2008.

[13] G. M. Burrowg and T. K. Gaylord, "Multi-beam interference advances and applications: Nano-electronics, photonic crystals, metamaterials, subwavelength structures, optical trapping, and biomedical structures," *Micromachines*, vol. 2, no. 2, pp. 221–257, 2011.

[14] C. Lu and R. H. Lipson, "Interference lithography: a powerful tool for fabricating periodic structures," *Laser Photon. Rev.*, vol. 4, no. 4, pp. 568–580, Jun. 2010.

[15] L. Xu, F. F. Luo, L. S. Tan, X. G. Luo, and M. H. Hong, "Hybrid plasmonic structures: Design and fabrication by laser means," *IEEE J. Sel. Top. Quantum Electron.*, vol. 19, no. 3, p. 4600309, 2013.

[16] Y.-J. Hung, P.-C. Chang, Y.-N. Lin, and J.-J. Lin, "Compact mirror-tunable laser interference system for wafer-scale patterning of grating structures with flexible periodicity," *J. Vac. Sci. Technol. B, Nanotechnol. Microelectron. Mater. Process. Meas. Phenom.*, vol. 34, no. 4, p. 040609, Jun. 2016.

[17] J. L. Stay, G. M. Burrow, and T. K. Gaylord, "Three-beam interference lithography methodology," *Rev. Sci. Instrum.*, vol. 82, no. 2, p. 23115, Feb. 2011.

[18] J. Xu, Z. Wang, Z. Zhang, D. Wang, and Z. Weng, "Fabrication of moth-eye structures on silicon by direct six-beam laser interference lithography," *J. Appl. Phys.*, vol. 115, no. 20, pp. 0–5, 2014.

[19] C. Liang, T. Qu, J. Cai, Z. Zhu, S. Li, and W.-D. Li, "Wafer-scale nanopatterning using fast-reconfigurable and actively-stabilized two-beam fiber-optic interference lithography," *Opt. Express*, vol. 26, no. 7, p. 8194, 2018.

[20] J. He, X. Fang, Y. Lin, and X. Zhang, "Polarization control in flexible interference lithography for nano-patterning of different photonic structures with optimized contrast," *Opt. Express*, vol. 23, no. 9, p. 11518, 2015.

[21] A. F. Lasagni, D. J. Yuan, and S. Das, "Layer-by-layer interference lithography of three-dimensional microstructures in SU-8," *Adv. Eng. Mater.*, vol. 11, no. 5, pp. 408–411, 2009.

[22] B. D. Gupta, A. M. Shrivastav, and S. P. Usha, "Surface plasmon resonance-based fiber optic sensors utilizing molecular imprinting," *Sensors (Switzerland)*, vol. 16, no. 9, 2016.

[23] Y. M. Kim and K. C. Choi, "Distortion Analysis of Periodic Ring Patterns Fabrication Using Surface Plasmon Interference Lithography With an Al Hexagonal Grating Structure on Glass," *IEEE Trans. Nanotechnol.*, vol. 17, no. 3, pp. 432–436, May 2018.

[24] A. G. Brolo, "Plasmonics for future biosensors," *Nat. Photonics*, vol. 6, no. 11, pp. 709–713, 2012.

[25] M. Seo, J. Lee, and M. Lee, "Grating-coupled surface plasmon resonance on bulk stainless steel," *Opt. Express*, vol. 25, no. 22, p. 26939, 2017.

[26] X. D. Hoa, A. G. Kirk, and M. Tabrizian, "Towards integrated and sensitive surface plasmon resonance biosensors: A review of recent progress," *Biosensors and Bioelectronics*, vol. 23, no. 2. pp. 151–160, 2007.

[27] C. Hu, "Surface plasmon resonance sensor based on diffraction grating with high sensitivity and high resolution," *Optik (Stuttg).*, vol. 122, no. 21, pp. 1881–1884, 2011.

[28] J. Dostálek and J. Homola, "Surface plasmon resonance sensor based on an array of diffraction gratings for highly parallelized observation of biomolecular interactions," *Sensors Actuators, B Chem.*, vol. 129, no. 1, pp. 303–310, 2008.

[29] K. Lin, Y. Lu, J. Chen, R. Zheng, P. Wang, and H. Ming, "Surface plasmon resonance hydrogen sensor based on metallic grating with high sensitivity," *Opt. Express*, vol. 16, no. 23, p. 18599, 2008.

[30] N. C. Y. Tham, P. K. Sahoo, Y.-J. Kim, and V. M. Murukeshan, "Ultrafast volume holography for stretchable photonic structures," *Opt. Express*, vol. 27, no. 9, pp. 12196–12212, 2019.

BIOS

Jian Yi Pae received the B.Eng (Hons.) degree in mechanical design engineering from the University of Glasgow in partnership with the Singapore Institute of Technology in 2016. He is currently pursuing the Ph.D degree in mechanical engineering from Nanyang Technological University (NTU), Singapore.

Since 2016, he is with the Singapore Centre for 3D Printing (SC3DP) and the Centre for Optical and Laser Engineering (COLE) as a Research Student. His research interests include laser interference lithography, optical biosensors, surface plasmon resonance and graphene-enhanced heterointerfaces.

Mr. Pae was awarded the NTU Research Student Scholarship for his Ph.D degree and also the Safety Systems Engineering Scholarship for his undergraduate studies.

Pankaj K. Sahoo received the B.Sc. & M.Sc. degree in physics from Utkal University, Odisha, India in 2008 and 2010 respectively. In 2012 he received the M.Tech. degree in applied optics with specialization in optics and photonics from the Indian Institute of Technology (IIT), Delhi, India. He then received the Ph.D. in physics from IIT, Delhi, India in October 2017. During the Ph.D. degree, he went to KTH, Stockholm, Sweden for a year under the Erasmus Mundus (India4EU II) program.

He was a research follow with NTU, Singapore from October 2017 to April 2019. He is currently a postdoctoral research associate with the Rochester Institute of Technology, N.Y., USA. His area of research is photonic crystals, resonant subwavelength grating structures, femtosecond laser-mater-interaction, surface plasmon resonance, light trapping for photovoltaic, biosensors, photonic circuits and light trapping in photovoltaic cells.

Murukeshan Vadakke Matham received the M.Sc. and M.Phil. degrees in Physics with specialization in quantum electronics from Cochin University of Science and Technology (CUSAT), India. He received the Ph.D. degree at the Indian Institute of Technology (IIT), Madras with the DAAD Fellowship Award to visit the University of Oldenburg, Germany.

He is an Associate Professor with the School of Mechanical & Aerospace Engineering, NTU, Singapore and is the Director of the COLE. Additionally, he is also the deputy director of The Photonics Institute (TPI) at NTU, Singapore. He has authored or co-authored more than 175 peer-reviewed papers in international journals and holds several patents and innovation disclosures in the area of applied optics and bio-optics. His research spans over biomedical optics, nanoscale optics, laser-based micro and nanofabrication, and optical metrology.

Dr. Murukeshan is the Associate Editor of the International Journal of Optomechatronics (IJO) and Editorial Board Member of Scientific Reports. He has guest edited international optics journal issues apart from being a regular reviewer for many leading optics journals. He is an SPIE-Visiting Lecturer and has given many lectures at universities and institutes under this program. He was the recipient of the prestigious Erudite Professorship from Kerala University, India in 2011. He is a Fellow of the Institute of Physics, UK.